Magnetic Induction Based Sensing and Localization for Fresh Food Logistics

Amitangshu Pal and Krishna Kant

Computer and Information Sciences, Temple University, Philadelphia, PA 19122

E-mail:{amitangshu.pal,kkant}@temple.edu

Abstract- Sensing of food spoilage and contamination is an active area of research, with many types of contact and non-contact sensors are being developed that can track fresh food quality throughout the distribution process. In this paper, we consider the communication of the sensed product quality along with the box position (in the stack of boxes in the truck or in a warehouse room) to the next level, in order to make the logistics more efficient and less wasteful. Given the water-rich, inhomogeneous biological media, RF or ultrasonic based communications are inappropriate in such environments, and we instead explore Magnetic Induction (MI) based communication framework in the HF band (3-30 MHz). We propose a novel magnetic induction based localization scheme to localize the boxes and study its accuracy via extensive simulations. We show that with a small number of anchor nodes, the localization can be done without any errors for boxes as small as 0.5 meter on the side, and with small errors even for boxes half as big. Our preliminary analysis suggests that such sensors can last for several years without any battery replacement.

I. INTRODUCTION

The purpose of this paper is to explore the use of magnetic induction (MI) based communication and localization to support advanced fresh food distribution logistics. MI refers to energy transfer between two inductor-capacitor (or LC) circuits, which is widely used in many areas, e.g. the charging of electric toothbrush, mobile phones, electric vehicles etc. [1]. In particular, we develop mechanisms to automatically monitor and report out the fresh food quality as measured by quality sensors enclosed in the boxes that may be stored in a distribution center or in transit in a truck, railcar, etc. The communicated quality along with the positional identification of the box can be exploited to trigger actions that can significantly reduce the fresh food waste, enhance distribution efficiency, and serve as early warning for contamination. These mechanisms would help develop the fresh food extension to the emerging concept of physical Internet [2].

It is well known that the presence of aqueous/tissue media of fresh food makes the use of normal RF communication (e.g., Bluetooth at the 2.4 GHz ISM band) and localization challenging due to high signal absorption and complex channel conditions [3]. Also RF based localization techniques can localize with the accuracy of few meters [4], which are not precise enough for localizing the shipping boxes of 0.5-1 meter dimension. Ultrasound (or acoustic) propagation in tissues is deeply affected by the highly inhomogeneous fresh

food media and leads to significant speed variations and multipath scattering [5]. Because of these limitations, we focus on magnetic induction (MI) based communications that are known to be less affected by such media. Compared to the RF-based techniques, the MI-based techniques have the following advantages: (a) better penetration performance (i.e., low absorption) as the magnetic permeability of tissue medium is very similar to that of air, (b) predictable channel conditions as MI communications are are less susceptible to surrounding environments, and (c) small coil antennas (e.g., a few mm or cm). The MI channels are also more determined as the MI signals are not reflected or scattered by the surrounding environments, and thus suffer from smaller signal fluctuations and multi-path effects [6].

Although magnetic induction based communications have been studied in the past for underground use [7], [8], their use for communication and localization is quite challenging in the context of fresh food logistics as discussed in the next section. We show that the proposed mechanism can achieve effective communication, accurate localization, and low power consumption. We exploit *the regular geometry of the shipping boxes and the information of their neighbor relationship* to develop a novel magnetic induction based localization scheme. Through simulations we show that using the proposed MI based localization scheme, the sensing devices can be located without any error for shipping boxes as small as 0.5 meter. We also show through preliminary analysis that such sensor nodes can operate for several years before needing any battery replacement. *To the best of our knowledge, we are the first to propose adopting the MI-based techniques for designing low-cost, low-power communication and localization mechanisms in the very challenging operating environment of food quality monitoring systems.*

The outline of the paper is as follows. Section II discusses the overall context of the research and its larger vision. Section III describes the suitability of MI communication in such environment as opposed to RF and ultrasonic. Section IV introduces the MI communication framework and discusses the channel model for it. Section V formulates the localization problem. In this section we show that the localization problem is NP-hard, and present a heuristic approach. Section VI shows extensive simulation results to explore the effectiveness of the mechanism. Section VII then concludes the discussion.

II. BACKGROUND AND MOTIVATION

Recently there are increasing expectations of "freshness" from the public and sustainability concerns that favor lo-

IEEE
computer
society

cally/regionally grown food and demand low-carbon footprint transportation and distribution. Unfortunately, the added freshness comes at the cost of more food waste, lower transportation efficiency, and higher carbon footprint. In particular, up to 40% of all food (and up to 50% of fresh food) is wasted in the US on its way from farm to table, which amounts to throwing away $165 Billion each year [9].

The inefficiency of private logistics has long been recognized and there is a definitive move towards 3rd party logistics (3PL) and its derivatives, which essentially outsources the logistics to a 3rd party that can serve multiple customers using common assets such as trucks, distribution centers, containers, etc. Another significant development is the borrowing of ideas from cyber Internet to create what is known as "Physical Internet" that includes modularized containers, standardized addressing mechanisms, shared logistics, etc. [10]. In this connection the authors in [2], [11] have examined Fresh Food Physical Internet (FFPI or $F^2\pi$) to integrate perishability into the physical Internet model. The third significant evolution is rapid automation of logistics including robotic processing, loading, unloading, positioning, self-driven vehicles, etc., often referred to as "Industry 4.0" initiative [12].

Automated sensing and communication of fresh food quality can play a central role in this landscape to reduce waste, increase efficiency, and enhance food safety. Our vision is that all packages of perishable products will have at least one sensing node that has a suitable array of sensors to detect crucial aspects of product quality including bacterial content, contamination, texture/color degradation, bruising, etc. Development of such sensors is currently a very active area and some simple sensors are already showing up, such as C_2Sense [13], FoodScan [14], Salmonella Sensing System [15] etc. Our focus is primarily in large boxes handled by the logistics, and these may contain one or more levels of smaller boxes, ultimately down to a package containing the product that can be sensed via various forms of contact (e.g., chemical) or non-contact (e.g., gas sampling, imaging) sensors. We envision at least one small package in the big box containing a sensor, though more could be deployed for better accuracy at a higher cost. The sensed quality needs to be communicated to a suitable decision maker or *Analytics & Operations Center (AOC)* for further analytics and action. The communication must be automatic (as opposed to someone opening the box and observing the sensor), should identify (or "localize") the box sending the sensed data, and the communication delay must be suitably bounded to provide maximum flexibility in corrective actions.

These observations provide the main motivation for our work, although in this paper we focus exclusively on the local communications part of the problem, i.e., communicating the sensed quality parameters to the "next level", which would be a truck, railcar, warehouse room, etc. Beyond this, the information can be communicated using existing technologies such as WiFi or Cellular. The main challenges in our communication and localization problems include (a) presence of very challenging communications media (e.g, water rich fruits/vegetables and meat tissue), (b) need for very low power
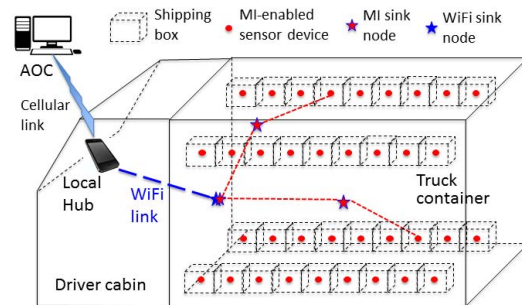
Fig. 1. A schematic diagram of the proposed network scenario.

and small size radios that do not require frequent battery change, and (c) potentially severe interference due to presence of many nodes in a small area (e.g., a truck or room full of product boxes, each with a sensor/radio as envisioned above).

III. DIFFERENT COMMUNICATION TECHNOLOGIES

Let us now consider the nature of the sensor radio suitable for such environment. Unfortunately, the presence of aqueous/tissue media of fresh food makes the use of normal RF communication (e.g., Bluetooth in the 2.4 GHz ISM band) challenging due to high signal absorption and complex channel conditions [3]. Reducing absorption by choosing lower frequencies (e.g., 802.11ah) helps in attenuation, but would need bigger antennas and cause severe interference in this very dense sensor environment. Authors in [16] show that in body-area-networks, especially in tissue medium, the path loss at 50 mm is 47-49 dB at 403.5 MHz. Other studies [17], [18] have also reported attenuation values ranging from 20 dB at 100 MHz to 60 dB at 1 GHz for distances less than 10 cm. High RF transmission powers are certainly undesirable because of serious overheating and thus quality loss [5].

Another promising technology in food or tissue medium is acoustic or ultrasonic communication. Ultrasonic waves are subject to lower absorption as compared to RF waves in aqueous or tissue medium. However, ultrasound (or acoustic) propagation [5] in tissues is deeply affected by multipath fading because of the inhomogeneity of the medium in terms of density and, consequently, sound velocity, and the pervasive presence of very small organs and particles. Therefore, numerous attenuated and delayed versions of the same transmitted signal reach the receiver, making detection and decoding a challenging operation. Also a significant portion of the energy is absorbed (although lower then RF) and converted into heat when ultrasounds propagate. This could potentially lead to a temperature increase, which will affect the quality of perishable food being transported.

Such challenges cannot be overcome until a major paradigm shift is made to address the limitations of current typical communication technologies in food medium. Prior research indicates that the Magnetic Induction (MI) based communication in the HF band (3-30 MHz) is largely unaffected by the tissue medium [19]. Compared to RF, MI suffers from smaller signal fluctuations and multi-path effects. The ability to use small coils (2.5/5.0cm in our experiments), short transmission

range (e.g., 1.5 m), and a decent data rate (e.g., 596 Kb/s) are ideal for our application. *Finally, ultra-low-power MI solutions consume less power than RF and ultrasound over short distances.* The MI channels are also more determined as the MI signals are not reflected or scattered by the surrounding environments, and thus suffer from smaller signal fluctuations and multi-path effects. Also there is no known biological effect of MI in the food or tissue medium.

		Indices
i, f, g, l	$\triangleq$	Index for sensor nodes and boxes (1, ..., N)
a	$\triangleq$	Index for anchors (1, ..., A)
		Variables
(r, ϕ, θ)	$\triangleq$	Radial distance, inclination and azimuth angle of the spherical coordinate system
μ	$\triangleq$	Permeability of the medium
ρ	$\triangleq$	Radius of the magnetic coils
$\mathbb{N}$	$\triangleq$	Number of turns of the magnetic coils
Δ	$\triangleq$	Box dimensions (i.e. length, height, width)
d_i^a	$\triangleq$	Distance of box-i from anchor-a
Pr_i^a	$\triangleq$	Power received at sensor node-i from anchor-a
x_{ig}	$\triangleq$	Whether or not the sensor node-i is in box-g
$\mathbb{S}_{if}^a$	$\triangleq$	Whether or not $Pr_i^a > Pr_f^a$
$\mathbb{B}_{gl}^a$	$\triangleq$	Whether or not the $d_g^a < d_l^a$
$\mathcal{I}_{\max}$	$\triangleq$	Maximum number of iterations of Algorithm 1

IV. MI BASED COMMUNICATION INFRASTRUCTURE

Fig. 1 shows the overall architecture where the shipping boxes are stacked in the container of a truck that carries fresh products. We assume that each shipping box carries multiple lowest level packages, i.e., a retail package of meat or a small package of fresh produce. *A sensing device is attached at one of the packages which is placed at the center of a shipping box.* Thus the sensed value of this device is considered as the representative of all the packages in that box. Even if Fig. 1 shows that the boxes are homogeneous and the truck is 100% full, the proposed scheme also works for boxes with different dimensions and partially full truckloads. Also instead of attaching the sensing device to the package at the center, it can be also be attached to the last package before closing the box (for packaging convenience). However the same protocol needs to be followed for all the boxes.

We assume that each sensor device is capable of both sensing and communication and is equipped with a low-cost MI radio operating at 10 MHz (which is the most commonly used frequency). We also assume that a few anchor-nodes with two radio interfaces (MI and WiFi) are mounted on the inner side of the truck container. The MI interface is for communication with the sensor devices, and the WiFi interface is for communication with the central controller in the driver cabin. The anchors also work as sinks to the sensing devices.

A. MI Based Channel Modeling

We use isotropic MI coil antennas consisting of three orthogonal coils to ensure reliable communications in all
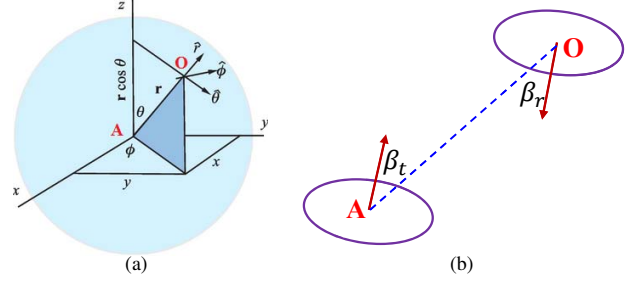
Fig. 2. (a) A spherical coordinate system where the receiver is located at O. (b) The intersection angle between two coils.

directions and thus robust localization. In particular it is no longer necessary to ensure that the coil planes of all radios are identical. We first discuss the magnetic field generated by a unidirectional coil using Fig. 2(a) and then extend that to develop orthogonal tri-directional coils. The relevant notations are enlisted in Table I. In Fig. 2, the transmitter is located at the origin A and the receiver is located at the observation point O, which is at a distance r away from the origin. The permeability of the medium is denoted by μ. The intersecting angles β_t and β_r in between the coils are determined as shown in Fig. 2(b). With these the magnetic field generated at the observation point O because of a unidirectional coil located at A, due to the current flowing of magnitude I_t is given by [20], [21], [22]

$$M_{t \to r} = \frac{\text{Flux} - \text{linkage}}{\text{current}} = \frac{\Phi_{t \to r}}{I_t}$$
$$\approx \frac{\mu \pi \mathbb{N}^2 \rho^4}{2r^3} \left| \cos\beta_t \cos\beta_r - \frac{1}{2}\sin\beta_t \sin\beta_r \right| \quad (1)$$

$\Phi_{t \to r}$ is the magnetic flux through the receiving coil C_r generated by C_t.

We now derive the expression of a tri-directional coil from the mutual inductances in between them. Notice that a tri-directional coil consists of three unidirectional coils that are orthogonal to one another. Because of this reason, the coils on the same sensor device do not interfere with each other. Assume that the transmitter has three orthogonal coils denoted as C_1, C_2 and C_3, whereas the receiver's are labeled with C_4, C_5 and C_6 respectively. Thus the mutual inductances between one of the transmitting coils (C_1, C_2 and C_3) and any of the three receiving coils (C_4, C_5 and C_6) can be given by $M_{u \to v}$ from equation(1) where $u = 1$, 2, or 3 and $v = 4$, 5, or 6. Since the induced current at the receiver can generate new magnetic field, there is a backward mutual inductance from the receiver to the transmitter. Usually, the mutual inductance is reciprocal, i.e. $M_{u \to v} = M_{v \to u}$.

Consider two coupled tri-directional coils (transmitter and receiver coils), assume that all 3 transmitting coils have the same voltage V_s. Let R_L denote the load resistance, C the capacitor needed to match with the coil's self-inductance L and is set to $C = \frac{L}{\omega^2}$ for ensuring resonant circuitry, where ω is the resonant frequency. Then the current in each of the coils (I_1 to I_6) can be derived by using Kirchhoffs voltage law as
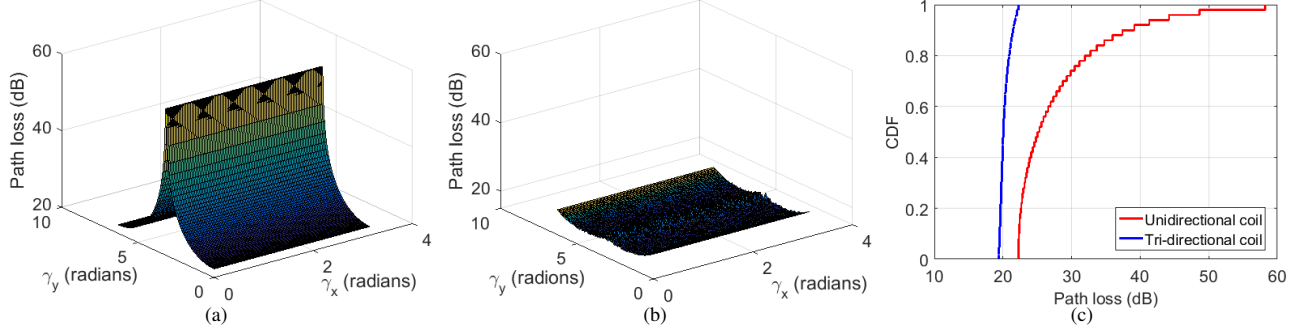
Fig. 3. (a) Path loss in case of unidirectional coil transceivers. (b) Path loss in case of tri-directional coil transceivers. (c) CDF of path loss for unidirectional coil and tri-directional coil transceivers. γ_x and γ_y denote the relative angle of the coils with respect to the x and y-axis respectively.
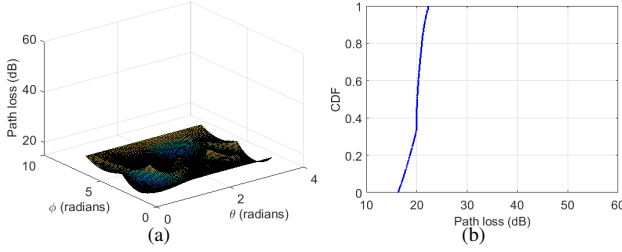
Fig. 4. (a) Path loss and its (b) CDF for tri-directional coil transceivers with different ϕ and θ.

Fig. 5. (a) Path loss with distance for tri-directional coil transceivers. (b) Received power with different source voltages.

follows:

$$
\begin{bmatrix} V_s \\ V_s \\ V_s \\ 0 \\ 0 \\ 0 \end{bmatrix} = \begin{bmatrix} R_L & 0 & 0 & X_{41} & X_{51} & X_{61} \\ 0 & R_L & 0 & X_{42} & X_{52} & X_{62} \\ 0 & 0 & R_L & X_{43} & X_{53} & X_{63} \\ X_{14} & X_{24} & X_{34} & R_L & 0 & 0 \\ X_{15} & X_{25} & X_{35} & 0 & R_L & 0 \\ X_{16} & X_{26} & X_{36} & 0 & 0 & R_L \end{bmatrix} \begin{bmatrix} I_1 \\ I_2 \\ I_3 \\ I_4 \\ I_5 \\ I_6 \end{bmatrix} \tag{2}
$$

where $X_{uv} = j\omega M_{u \to v}$. With these the path loss can be expressed by

$$
\mathbb{L} = -10\log\frac{\mathcal{P}r}{\mathcal{P}t} = -10\log\frac{\sum_{u=4}^{6} |I_u|^2 R_L}{\sum_{u=1}^{3} \Re(V_s I_u)} \tag{3}
$$

where $\mathcal{P}t$ and $\mathcal{P}r$ are the power transmitted and received respectively. $\Re(q)$ represents the real value of a complex variable q.

Fig. 3 shows the comparison of unidirectional and tri-directional coil transceivers with different coil orientations. μ and $\mathbb{N}$ are assumed to be $4\pi \times 10^{-7}$ Henrys/m and 10 respectively. We keep $r = 1$ meter and the source voltage $V_s = 3$ V in Fig. 3. R_L is assumed to be of 1Ω. In Fig. 3, we keep the coil position fixed and change the coil orientations with respect to its x and y axis. Notice that for the tri-directional coil, the orientations (γ_x and γ_y) in Fig. 3(a)-(b) denotes the orientation of one of the three unidirectional coils. The other two coil's orientation vary with respect to the first one, such that all there are orthogonal. From this figure we can observe that with tri-directional coil transceivers the transmission characteristics is near-isotropic which makes it suitable for our application. Also the tri-directional coil has lower path loss compared to the unidirectional coil as seen

from Fig. 3(c). We next keep the receiver coil orientation fixed, and change its relative position in the 3D space by varying the θ and ϕ in Fig. 1(a). The result is shown in Fig. 4, where r is assumed to be of 1 meter. From this figure we can observe that as far as the distance in between the coils are the same, their relative position in the 3D space do not affect the received signal strength in between them.

Fig. 5(a) shows the path loss with distance using tri-directional coil transceivers. From this figure we can observe that with $V_s = 3$ V, the transmission range of tri-directional coil transceivers are typically 2-3 meters (considering 70 dB of loss) with $\rho = 0.025$ meter and even higher with larger coil radius, which is adequate for our applications.

However in a network of multiple nodes, there will be multiple such tri-directional coils with interdependent mutual inductances in between them. The mutual inductances in between any two coils can be calculated using equation(1), which can be utilized to calculate the current at each one of the coils using the similar approach as in equation(2). Thus the power received at each node is calculated by adding the received power in its three coils.

B. MI Based Communications

Since the MI-based communication has a short transmission range, multi-hop communication will be a must when there is no direct link between a sensor device and its nearest sink-node. Hence, a data-gathering tree/forest needs to be constructed (or reconstructed) when the network is formed (or changed) so that each sensor device has a path to its nearest sink-node. This can be done using the existing schemes from the rich literature of research on wireless sensor networks (e.g.,

[23]). Fig. 6(a) shows the effect of multi-hop magnetic communication with different number of link-level retransmissions (η) and number of hops (Ψ). We assume link-level packet error rate $P_e = 10^{-3}$, which is obtained from experimental results in [24] for a 1-1.5 meter magnetic link. From Fig. 6(a) we can observe that the packet delivery ratio (i.e. $(1 - P_e^\eta)^\Psi$) is more than 99% even with 10 hops, which shows the feasibility of multi-hop communication in such environment. Note that since low-power communication is a critical requirement here, the data-gathering tree/forest will need to be constructed in a way that minimizes the energy consumption (e.g., this can be approximated by minimizing the total number of data transmissions).
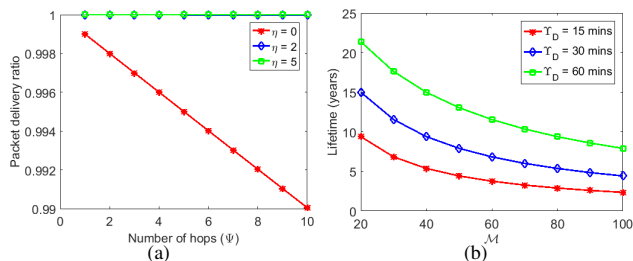
Fig. 6. (a) Packet delivery ratio and (b) lifetime of the sensor nodes for multi-hop communication.

Due to the near-field transmissions via the coupled magnetic field, the receiver coil can detect the MI signal without actively "listening". Hence, an MI signal intended for a nearby sensor device may also be detected. Thus an ultra-low-power wake-up component can be integrated, which triggers up the communication module when an MI signal is detected. The communication module remains in sleep mode most of the time and will be periodically (e.g., once every 15-30 minutes) woken up for reporting the sensed data, or when triggered by the wake-up component. In such low-power modes the sensor devices are mostly inactive and can run for several years without any battery change. For example with power consumption of 1.5 mW@1V [25] in the active mode, a sensing device can last for several years with a chip battery of 220 mAh [26] if it operates in $\sim$1% duty cycle. In general the power consumption in each node is represented as:

$$P = \frac{P_{Bt}T_{Bt}}{\Upsilon_B} + \mathcal{N}\frac{P_{Br}T_{Br}}{\Upsilon_B} + \mathcal{M}\frac{P_{Dt}T_{Dt}}{\Upsilon_D} + \mathcal{R}\frac{P_{Dr}T_{Dr}}{\Upsilon_D} + A\frac{P_{Dr}T_{Dr}}{\Upsilon_L} + \frac{P_s T_s}{\Upsilon_S}$$

where P_x and T_x represent the power consumption and the duration, respectively, of the event x; and Υ_B, Υ_D and Υ_S represent the beacon interval, data interval and sampling interval respectively. Transmission/reception of beacons is denoted by B_t/B_r, data transmit/receive is denoted by D_t/D_r, and sensing is denoted as S, respectively. $\mathcal{N}$ is the number of neighbors, $\mathcal{M}$ and $\mathcal{R}$ are the number of sensor nodes whose packets are forwarded and received/overheard by the node respectively. We assume that there are A anchor nodes that transmit control messages (for localization or sending other updates) with an interval of Υ_L.

Fig. 6(b) shows the lifetime of such a sensor node with $\mathcal{N}$ = 20, $\mathcal{A}$ = 12, and $\mathcal{M} = \mathcal{R}$. Υ_B and Υ_L are assumed to be

30 minutes and 1 hour respectively. We assume that the radios remain on for 15 ms for reception and forwarding, which is sufficient to transmit/receive packets with a data rate of 596 Kbps [25]. Notice that in Fig. 6(b) we only consider power consumption due to communications (i.e. transmissions and receptions). Actually the lifetime will be sightly less due to power consumption due to sensing, however food sensors like C_2Sense consumes $\sim 10\mu$W for sensing [27] which is several orders of magnitude lesser than the communication module. Also Fig. 6(b) gives a conservative estimate of the battery lifetime, which can be further stretched by implementing event-driven sampling and communication (i.e. transmit when the change in quality is more than some threshold) rather than doing it periodically. Also in reality, $\mathcal{M}$ is not going to be more than 50 in a truck environment with 100-200 boxes, which ensures that a sensor node can last even more than 5 years without any battery replacement. Although battery-free energy-harvesting devices can be alternative solutions, we do not consider integrating them here due to their higher cost and variability in the harvested energy.

V. MI Based Localization Scheme

We assume that the box positions are precisely known to the central controller which is possible in the future, advanced food logistics where the loading-unloading of the shipping boxes will be done in an automated fashion for better and well-planned truck space utilization. However in a large food chain it is hard to keep track of which sensor is in which box. Thus the purpose of our localization is to identify from which box the sensed data is coming, or to identify the shipping boxes with products that may have contamination or spoilage.

A. A Conceptual Overview

Ideally for localizing the sensor nodes we need to estimate their distances from some reference points (or anchors). However in presence of multiple such nodes, their interdependent mutual inductances make the distance estimate highly erroneous. Also the distance estimate requires precise knowledge of the channel parameters which is hard to obtain in our applications, as they vary depending on the types of the food products or whether the truck (or boxes) are fully loaded or not etc. The distance estimate also requires the exact orientations of the coils, which is also not available in this scenario as different food packages can be kept in different orientations while packing them to the boxes. In case of MI communication, the distance estimate is also disturbed by the ferromagnetic materials inside the truck walls. Therefore in contrast to such distance based localization mechanisms [22], [8], our objective is to collect the information of the received power at the sensor nodes from an anchor to get their relative distance with respect to that anchor and use this information to localize them to the known box positions. We argue in section V-D that such an approach is robust even in presence of the truck walls.

We explain this with the help of Fig. 5(b) where we deploy 5 cubic boxes with dimensions (Δ) equal to 1 meter side by

side. A sensor node is placed at the center of each box. We assume that there is one anchor that transmits pilot signals whose received power is recorded by the 5 sensor nodes. Box-1 is closest to the anchor whereas box-5 is the farthest. Fig.5(b) shows that variation of the received powers at the sensor nodes with different voltage V_s. From this figure we can observe that the received power is monotonically increasing function of V_s, also the relative order of the received power at different sensor nodes remain consistent with different V_s. We can also observe that the received powers are consistent with the box distances from the anchor, i.e. the received power of sensor node-1 is the highest whereas that of node-5 is the lowest. Thus we can maintain a constant V_s at an anchor and can get a relative order of the other node's positions which can be matched to that of the boxes. However as the received power is the function of the mutual effect of all the node's coils, the order can also be disturbed in presence of higher number of sensor nodes. The relative order can also be disturbed as the propagation characteristics is not completely isotropic, as obtained from Fig. 3(b)-(c).

In order to study the impact of many sensors, we develop a factor called *outlier factor* which is defined as follows. Consider a scenario where N boxes (along with sensing devices) are placed in a 3-D grid such that the i-th sensor node is placed in the i-th box. An anchor is placed at one corner of the grid with enough power to reach all nodes. We assume that $\mathbb{S}_{ig}$ is an adjacency matrix which is 1 if the received power of sensor node-i is more than that of g, and $\mathbb{B}_{ig}$ is 1 if box-i is closer to the anchor than box-g. With this the outlier factor is equal to $\frac{\sum_i \sum_g |\mathbb{S}_{ig} - \mathbb{B}_{ig}|}{\sum_i \sum_g \mathbb{S}_{ig}}$. Thus the outlier factor measures the level of inconsistencies between the power received by the sensor nodes and their corresponding box distances from the anchor. For example in Fig. 5(b) the outlier factor is 0, as the received power is consistent with the box distances from the anchor.

Fig. 7 shows the variation of the outlier factor with different Δ. We consider two cases, one with 3-D grid of $5\times5\times5$ boxes and the other with $10\times5\times5$ boxes. From Fig. 7 we can observe that even with $\rho = 0.05$ meter and $\Delta = 0.5$ meter, the outlier factor remains below 0.4 with both in case of 125 and 250 sensor nodes, i.e. less than 40% of the relative ordering are inconsistent whereas the rest are consistent. However the outlier factor is significantly low (below 0.2) when the coil radius $\rho = 0.025$ meter. From this point onwards we therefore keep the coil radius $\rho = 0.025$ meter because of its smaller outlier factor and thus for better localization accuracy. The transmission range with $\rho = 0.025$ meter is 2-3 meters which is adequate for our purpose. The small size of such coils makes it easier to be attached in small food products as well.

B. Localization Problem Formulation

We assume that there are N sensor nodes that are placed in N shipping boxes. A anchors are placed at different corners at the trucks (or warehouses) whose transmissions can be received by all the sensor nodes. This assumption is feasible as the anchors are not battery constrained and
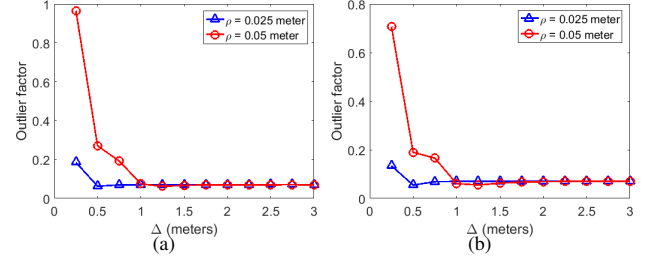
Fig. 7. Variation of outlier factor with different Δ, in case of (a) 125 sensor nodes, and (b) 250 sensor nodes.

thus use higher V_s to extend their transmission ranges. Each anchor transmits a *pilot* signal separately (i.e. two anchors do not transmit at the same time). The sensor nodes record the received power corresponding to the pilot signals from different anchors and report them to the sinks (which report them to the central controller through WiFi interface) using multi-hop communications as discussed in section IV-B. The localization is done at the central controller which knows the box locations and thus the relative order of the boxes from each anchor. It also records the relative distance order of the sensor nodes from each anchor based on their received power from the anchors. With these we now formulate our magnetic localization problem, that assigns the sensor nodes to the boxes based on the received power measurements of the sensor nodes as well as the known distance order of the boxes from the anchors. Assume that x_{ig} is a binary decision variable which is 1 if node-i is assigned to box-g. Also assume that d_i^a denotes the distance between anchor-a and the box-i. $\mathbb{S}_{if}^a$ is an input binary variable which is 1 if $Pr_i^a > Pr_f^a$, and $\mathbb{B}_{gl}^a$ is also an input binary variable if box-g is closer to a than box-l, i.e. $d_g^a < d_l^a$. With these the problem can be formulated as follows:

$$\text{Maximize} \quad \sum_{a=1}^{A}\sum_{i=1}^{N}\sum_{g=1}^{N}\sum_{f=1}^{N}\sum_{l=1}^{N} x_{ig}x_{fl}\mathbb{S}_{if}^a\mathbb{B}_{gl}^a \quad (4)$$

$$\text{subject to} \quad \sum_{g=1}^{N} x_{ig} = 1, \quad \forall i \in \mathscr{S} \quad (5)$$

$$\sum_{i=1}^{N} x_{ig} = 1, \quad \forall g \in \mathscr{B} \quad (6)$$

$$x_{ig} \in \{0,1\} \quad \forall i \in \mathscr{S}, g \in \mathscr{B} \quad (7)$$

where $\mathscr{S}$ and $\mathscr{B}$ are the set of sensor nodes and boxes. The objective is to assign the sensor nodes into the boxes such that the similarities in between the distance order of the sensor nodes and the boxes are maximized. For example assume that the sensor node-i is assigned to box-g, and the sensor node-f is assigned to box-l. In such a scenario, if $Pr_i^a > Pr_f^a$ and $d_g^a > d_l^a$, then $\mathbb{S}_{if}^a = 1$ and $\mathbb{B}_{gl}^a = 0$. Thus the expression $x_{ig}x_{fl}\mathbb{S}_{if}^a\mathbb{B}_{gl}^a$ becomes 0, or there is a discrepancy in the distance orders corresponding to this assignment. On the other hand if $d_g^a < d_l^a$, then $x_{ig}x_{fl}\mathbb{S}_{if}^a\mathbb{B}_{gl}^a$ equals to 1, which says that the assignment conforms the corresponding distance orders. Constraints(5-6) ensure that a sensor node is assigned to exactly one box and vice versa.

388

Theorem 1. *The problem of magnetic localization is NP-hard.*

Proof: We first define the *largest common subgraph* problem (LCS) which is known to be NP-complete. Graph H is said to be *common* to graphs G_1 and G_2 if both G_1 and G_2 contain induced subgraphs isomorphic to H. The maximum common subgraph problem can be defined as follows: given a pair of graphs G_1 and G_2, find the largest induced subgraph common to both.

We now show that our magnetic localization problem contains the largest common subgraph problem as a special case. Assume an instance of the magnetic localization problem with $A = 1$, then $\mathbb{S}^1$ and $\mathbb{B}^1$ are two $N \times N$ adjacency metrices. We construct two directed graphs $\mathbf{U}$ and $\mathbf{V}$ such that $U_{ig} = \mathbb{S}^1_{ig}$ and $V_{ig} = \mathbb{B}^1_{ig}$.

Then a graph H is the largest common subgraph of $\mathbf{U}$ and $\mathbf{V}$ if and only if the maximum value of equation(4) is equal to the number of edges in H. This can be verified by using the rectangle rule of subgraph isomorphism as mentioned in [28], i.e. when $x_{ig} = x_{fl} = U_{if} = V_{gl} = 1$ in (4) it forms a rectangle as shown in Fig. 8. Thus finding the maximum of (4) is equivalent to finding the

Fig. 8. Rectangle rule for subgraph isomorphism. The red and green vertices are the vertices of graphs $\mathbf{U}$ and $\mathbf{V}$ respectively.

number of such rectangles. This is equivalent to finding the maximum number of common links of $\mathbf{U}$ and $\mathbf{V}$, or in turn solving the largest common subgraph problem. Since the largest common subgraph problem is NP-complete and a special case of the magnetic localization problem, thus our magnetic localization problem is NP-hard. ∎

C. Proposed Heuristic

As the problem is NP-hard we propose a heuristic solution for assigning the sensor nodes to the boxes, which is discussed in Algorithm 1. The idea is to consider $\mathbb{S}^a$ and $\mathbb{B}^a$ as two directed graphs, and then to best match the vertices of these two graphs. We thus propose a graph matching scheme which is inspired by [28]. We first modify the objective function of equation(4) $E = \sum_{a=1}^{A} \sum_{i=1}^{N} \sum_{g=1}^{N} \sum_{f=1}^{N} \sum_{l=1}^{N} x_{ig} x_{fl} \mathbb{S}^a_{if} \mathbb{B}^a_{gl}$ using Taylor series expansion as follows:

$$
\begin{aligned}
E &= \sum_{a=1}^{A} \sum_{i=1}^{N} \sum_{g=1}^{N} \sum_{f=1}^{N} \sum_{l=1}^{N} x_{ig} x_{fl} \mathbb{S}^a_{if} \mathbb{B}^a_{gl} \\
&\approx \sum_{a=1}^{A} \sum_{i=1}^{N} \sum_{g=1}^{N} \sum_{f=1}^{N} \sum_{l=1}^{N} x^0_{ig} x^0_{fl} \mathbb{S}^a_{if} \mathbb{B}^a_{gl} + \sum_{i=1}^{N} \sum_{g=1}^{N} Q_{ig} \left(x_{ig} - x^0_{ig} \right)
\end{aligned}
\tag{8}
$$

where $Q_{ig} = \frac{\partial E}{\partial x_{ig}} \Big|_{x_{ig}=x^0_{ig}} = \sum_{a=1}^{A} \sum_{f=1}^{N} \sum_{l=1}^{N} x^0_{fl} \mathbb{S}^a_{if} \mathbb{B}^a_{gl}$.

In equation(8) x^0_{ig} is assumed to be the initial estimate of x_{ig}. Thus maximizing the above Taylor expansion is equivalent to maximizing $\sum_{i=1}^{N} \sum_{g=1}^{N} Q_{ig} x_{ig}$, which is an *assignment*
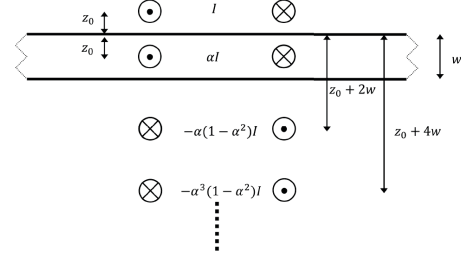
Fig. 9. Methods of images [30].

problem and can be solved by using the *Hungarian assignment* scheme [29]. We thus propose an iterative procedure as follows: we first start with an initial value of x_{ig} and expand the first order Taylor series by taking the partial derivative to calculate Q_{ig}. We next use the Hungarian scheme corresponding to that Q_{ig} to get an initial assignment. This assignment or x_{ig} is next used to calculate the modified Q_{ig} from equation(8). This process is repeated until the solution converges or a maximum number of iterations $\mathcal{I}_{\max}$ is reached.

Algorithm 1 Assignment scheme from the sensor nodes to individual boxes

---

1: INPUT : A number of anchors, $\mathbb{S}^a$ order matrix of the sensor nodes corresponding to anchor-a, $\mathbb{B}^a$ order matrix of the boxes corresponding to anchor-a, $\mathbb{M}$ is a large number.
2: OUTPUT : Assignment of the sensors to the boxes.
3: x^0 is initialized to any random assignment matrix;
4: **while** x is not converged or number of iterations $< \mathcal{I}_{\max}$ **do**
5:     $Q_{ig} = \sum_{a=1}^{A} \sum_{f=1}^{N} \sum_{l=1}^{N} x^0_{fl} \mathbb{S}^a_{if} \mathbb{B}^a_{gl} \ \forall \ i, g$;
6:     Use Hungarian method with cost $c_{ig} = \mathbb{M} - Q_{ig}$ to get an assignment x_{ig};
7:     $x^0_{ig} = x_{ig}, \ \forall \ i, g$;
8: **end while**

D. Effects of the truck walls

Localization of boxes carried on a carrier (e.g., truck) may be thwarted by the ferromagnetic (mild steel) materials inside walls of truck since the anchors will be mounted on those walls. Suppose that an anchor coil (with current I) is placed at a distance z_0 from the truck wall. Then the key question is how this wall distorts the magnetic field, and what errors would it introduce in localization? Our preliminary theoretical analysis suggests – rather surprisingly – that the wall will not have a detrimental effect for the localization accuracy of our proposed scheme, but this needs to be investigated further. The key to analyzing this situation is the classical *image theory*, which suggests that a ferromagnetic wall of finite width w will result in an infinite number of mirror coil images as shown in Fig. 9 [30]. There will be a mirror image at $-z_0$ with current αI, which we call primary image. In additional to that there will be infinite number of secondary image coils carrying a current $\alpha^{2n-3}(1-\alpha^2)I$, for $n \geq 2$. Each of these mirror coils will be found at a distance $z = -(2nw+z_0)$. Here $\alpha = \frac{\mu_r-1}{\mu_r+1}$, where μ_r is the relative permeability of the truck material.

Using this phenomenon, we argue that the relative ordering of sensors (derived from signal strength) will remain unchanged. This is because the relative permeability μ_r for such ferromagnetic materials is very high, exceeding 1000, which means $\alpha \sim 1$. Thus the effects of the secondary images
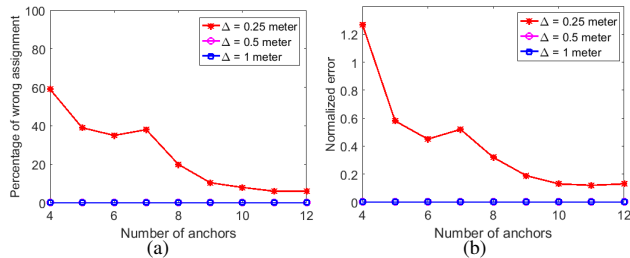
Fig. 10. (a) Percentage of wrong assignment when 125 boxes are kept in a 5×5×5 grid, and the (b) corresponding average normalized error.
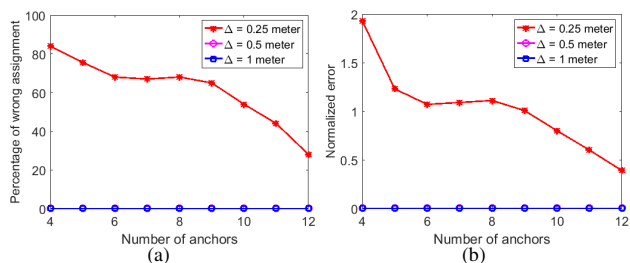
Fig. 11. (a) Percentage of wrong assignment when 250 boxes are kept in a 10×5×5 grid, and the (b) corresponding average normalized error.

become insignificant, and moreover, the primary image helps strengthen the anchor signal. These results really apply to infinite, perfectly smooth walls, and real conditions may cause some difficulties (e.g., at the corners) which is subject to further investigations. However the presence of the ferro-magnetic objects makes our proposed localization scheme particularly apt[1], rather then the distance based localization schemes studied in [22], [8]. On the other hand for the trucks with wooden walls, the relative permeability becomes so low that the effect of walls become insignificant, i.e. a wooden wall hardly induces any eddy current from the nearby current carrying objects.

VI. PERFORMANCE EVALUATIONS

We study the accuracy of the proposed MI based localization scheme using Matlab simulations. The simulated system topology along with the anchor's placement is similar to that in Fig. 1. We simulate two cases: in the first case 125 boxes are placed in a 5×5×5 grid, whereas in the second environment we consider 250 boxes placed in a 10×5×5 grid. The boxes are assumed to be cubic and symmetric with dimension Δ, however the proposed scheme is equally applicable for boxes with different dimensions. We assume the minimum Δ to be 0.25 meter as the worst case scenario, however in reality the boxes are even more the 0.5-1 meter. We record two indicators to analyze the accuracy of the proposed scheme. The first indicator is the percentage of sensor nodes that are assigned in wrong boxes by our localization scheme. The second indicator is the normalized error which is equal to

---

[1]Our proposed localization scheme is also application when all the nodes have identical orientations, which is possible for a more futuristic, completely automated packing environment. Notice that in case of identical node orientations, a single coil (instead of 3-coils) can also be used for successful communication and localization.

$\left(\dfrac{\text{distance error between actual and prescribed box centers}}{\Delta} \right)$.
The normalized error gives an estimation that if a spoiled package is not found in its prescribed box, then how many neighboring boxes need to be searched to find that package.

A. Results for 125 boxes

Fig. 10(a)-(c) show the accuracy of the proposed scheme in case of 125 boxes. From Fig. 10(a) we can observe that the percentage of wrong assignment is zero as far as Δ is more than or equal to 0.5 meter. In case of $\Delta = 0.25$ meter the amount of wrong assignment reduces by $\sim$55% as the number of anchors increase from 4 to 12. Fig. 10(b) shows the average normalized error with different number of anchors and Δ. When the number of anchors is less than 5, the percentage of wrong assignment is above 40% with $\Delta = 0.25$ meter as seen from Fig. 10(a). However even in such cases the average normalized error is less than 2, i.e. the targeted box can be found within 2 boxes in the neighborhood of the prescribed box. The average normalized error reduces by $\sim$85% when the number of anchors is increased from 4 to 12.

B. Results for 250 boxes

Fig. 11 shows the performance of the proposed scheme for 250 boxes. From Fig. 11(a) we can observe that with $\Delta = 0.25$ meter, the percentage of wrong assignment is significantly high when the number of anchors is low. However the average normalized error is still less than 2 in all cases. The amount of miss-assignment is reduced significantly ($\sim$50%) when the number of anchors is increased from 4 to 12. We have also observed that with 12 anchors and $\Delta = 0.25$ meter (not shown in the figures), for more than 90% of the sensor nodes the normalized error is less than 1, even the maximum error is less than 2.

The percentage for wrong assignment is significantly lower and goes to zero as long as the Δ is more than or equal to 0.5 meter. In all of these scenarios, the sensor nodes are localized with sufficiently high level of accuracy as far as Δ is more than or equal to 0.5 meter. In reality large boxes carrying multiple small packages are indeed more than 0.5-1 meter, thus the proposed scheme can be effectively useful in the real world food logistics with reasonable accuracy to localize and isolate the nearly spoiled or contaminated boxes.

C. Comparison with RF localization scheme

We next compare our proposed localization scheme with a hypothetical isotropic RF scenario. For RF channel modeling we assume a log-normal shadowing model to calculate the path loss; the path loss exponent and standard deviation of the log-normal fading model for tissue medium is assumed to be 4.26 and 6 dB respectively [16], [31]. The reference distance loss at 50 mm is assumed to be 49.81 dB. The path loss exponent is assumed to be known and is used to calculate the distance estimation in between the sensor nodes and the anchors. This distance estimate is used in a multilateration scheme [32], [33] to calculate the estimated positions of the sensor nodes. We construct a bipartite graph of N sensor nodes and boxes, with
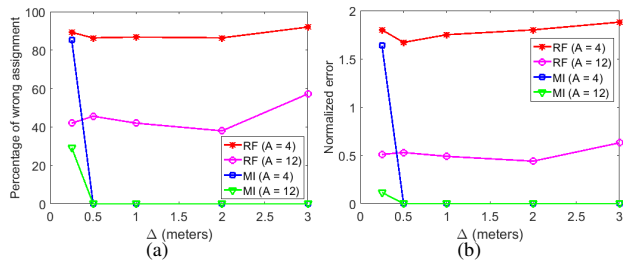
Fig. 12. Comparison of RF and MI based localization schemes: (a) percentage of wrong assignment, and (b) average normalized error with different Δ.

the edges (or costs) in between them representing the distance between the estimated position of the sensor nodes and the box centers. We next implement the Hungarian scheme to assign the sensor nodes to individual boxes.

Fig. 12 shows the comparison of the proposed MI based and RF localization schemes in presence of 4 and 12 anchors respectively. We assume 250 sensor nodes (or boxes) in this case. From Fig. 12 we can observe that in case of RF the localization accuracy does not improve with the increase in Δ. The reason is mainly because of the shadowing effects which disturb the RSSI of the individual sensor nodes. On the other hand in case of magnetic communications, the localization accuracy improves significantly and goes to zero as the Δ increases due to smaller number of outliers as observed from Fig. 7.

VII. CONCLUSIONS

In this paper, we developed a sensing and localization mechanism for MI-based communications in fresh food transportation environments. We first described an isotropic magnetic communication framework so that the signal can be received at all directions irrespective of the orientations of the sensor antennas. By considering the unknown orientations and channel models in food transportation environments, we proposed a localization scheme for the sensor nodes in individual boxes carrying perishable food packages. The major outcome of the simulation experiments is the fact that the sensor nodes are localized with acceptable accuracy as far as the box lengths are more than 0.5 meter or above. We also show that such sensor nodes can last for several years without any battery replacement. As stated in section II, simple and inexpensive sensors are already beginning to show up in retail meat packages. Therefore, an important line of investigation is to consider future scenarios where the entire sensor module (including the radio) is inexpensive enough to be embedded in each package or multiple packages within a box. We also plan to develop experimental setup to validate the performance of the proposed sensing and localization scheme in a real-world scenarios. We will study the effects of metallic walls on the accuracy of the proposed localization scheme using such setup.

REFERENCES

[1] X.Mou *et al.*, "Wireless power transfer: Survey and roadmap," in *IEEE VTC*, 2015, pp. 1–5.
[2] A.Pal *et al.*, "F$^2\pi$: A physical internet architecture for fresh food distribution networks," in *IPIC*, 2016.
[3] R.Jedermann *et al.*, "Communication techniques and challenges for wireless food quality monitoring," *Philosophical Transactions of the Royal Society*, vol. 372, p. 20130304, 2014.
[4] H.Liu *et al.*, "Survey of wireless indoor positioning techniques and systems," *IEEE Trans. Systems, Man, and Cybernetics, Part C*, vol. 37, pp. 1067–1080, 2007.
[5] G. E.Santagati *et al.*, "Ultrasonic networking for e-health applications," *IEEE Wireless Commun.*, vol. 20, 2013.
[6] "The NFMI chip creates a low-power magnetic field around devices and uses the attractive forces to transfer voice and data," http://www.freelinc.com/technology/.
[7] Z.Sun *et al.*, "Magnetic induction communications for wireless underground sensor networks," *IEEE Transactions on Antennas and Propagation*, vol. 58, pp. 2426–2435, 2010.
[8] X.Tan *et al.*, "On localization for magnetic induction-based wireless sensor networks in pipeline environments," in *IEEE ICC*, 2015, pp. 2780–2785.
[9] D.Gunders, "Wasted: How america is losing up to 40 percent of its food from farm to fork to landfill," 2012.
[10] B.Montreuil, "Towards a physical internet: Meeting the global logistics sustainability grand challenge," *Logistics Research*, vol. 3, pp. 71–87, 2011.
[11] K.Kant *et al.*, "Internet of perishable logistics," *IEEE Internet Computing*, vol. 21, pp. 22–31, 2017.
[12] M.Hermann *et al.*, "Design principles for industrie 4.0 scenarios," in *HICSS*, 2016, pp. 3928–3937.
[13] "C$_2$Sense," http://www.c2sense.com.
[14] http://www.israel21c.org/keeping-food-safe-from-farm-to-fork/.
[15] "Salmonella sensing system: New approach to detecting food contamination enables real-time testing," http://phys.org/news/2013-10-salmonella-approach-food-contamination-enables.html.
[16] I.Dove, "Analysis of radio propagation inside the human body for in-body localization purposes," August 2014. [Online]. Available: http://essay.utwente.nl/66071/
[17] D.Werber *et al.*, "Investigation of rf transmission properties of human tissues," 2006.
[18] H.-Z. T.Chen *et al.*, "A study of rf power attenuation in bio-tissues," vol. 24, pp. 141–146, 2004.
[19] M.Masihpour *et al.*, "Multihop relay techniques for communication range extension in near-field magnetic induction communication systems," *Journal of Networks*, vol. 8, pp. 999–1011, 2013.
[20] H.Guo *et al.*, "Channel modeling of MI underwater communication using tri-directional coil antenna," in *IEEE GLOBECOM*, 2015, pp. 1–6.
[21] C. A.Balanis, *Antenna Theory: Analysis and Design*. Wiley-Interscience, 2005.
[22] X.Tan *et al.*, "Environment-aware indoor localization using magnetic induction," in *IEEE GLOBECOM*, 2015, pp. 1–6.
[23] Y.Wu *et al.*, "Constructing maximum-lifetime data gathering forests in sensor networks," *IEEE/ACM Transactions on Networking (TON)*, vol. 18, pp. 1571–1584, 2010.
[24] X.Tan *et al.*, "A testbed of magnetic induction-based communication system for underground applications," *CoRR*, 2015.
[25] "NXP Introduces Ultra-low Power Radio Transceiver Enabling Wireless Earbuds," http://www.everythingrf.com/News/details/1399-nxp-introduces-ultra-low-power-radio-transceiver-enabling-wireless-earbuds.
[26] "Lithium Batteries & Coin Cells," https://learn.adafruit.com/all-about-batteries/lithium-batteries-and-coin-cells.
[27] http://ucanr.edu/datastoreFiles/234-2824.pdf.
[28] S.Gold *et al.*, "A graduated assignment algorithm for graph matching," *IEEE Trans. Pattern Anal. Mach. Intell.*, vol. 18, pp. 377–388, 1996.
[29] H. W.Kuhn, "The hungarian method for the assignment problem," *Naval Research Logistics Quarterly*, vol. 2, pp. 83–97, 1955.
[30] K.ODonoghue *et al.*, "Planar magnetic shielding for use with electromagnetic tracking systems," *IEEE Transactions on Magnetics*, vol. 51, pp. 1–12, 2015.
[31] K.Sayrafian-Pour *et al.*, "A statistical path loss model for medical implant communication channels," in *IEEE PIMRC*, 2009, pp. 2995–2999.
[32] A.Norrdine, "An algebraic solution to the multilateration problem," in *(IPIN)*, 2012.
[33] A.Wessels *et al.*, "Dynamic indoor localization using multilateration with rssi in wireless sensor networks for transport logistics," *Procedia Engineering*, vol. 5, pp. 220–223, 2010.